Synthesis, Structure, and Catalytic Properties of the Layered Oxide $SbOReO_4 \cdot 2H_2O$: Location of Hydrogen-Atom Positions by Powder Neutron Diffraction

William T. A. Harrison*

Department of Chemistry, University of Houston, Houston, Texas 77204-5641

Adrian V. P. McManus

Chemical Crystallography Laboratory, University of Oxford, Oxford OX1 3PD, England

Mark P. Kaminsky

Amoco Chemical Company, P.O. Box 400, Naperville, Illinois 60566

Anthony K. Cheetham*

Materials Department, University of California, Santa Barbara, California 93106-9050

Received April 23, 1993. Revised Manuscript Received August 5, 1993®

A new hydrated antimony rhenium oxide, $SbOReO_4 \cdot 2H_2O$, has been prepared by hydrothermal methods and fully characterized by powder neutron diffraction. The structure consists of double layers built up from infinite, interconnected arrays of $[SbO^+]_n$ and ReO_4^- units. Water molecules reside in the interlamellar region, and all four protons are involved in hydrogen bonds which are responsible for holding the structure together. Catalytic activity of dehydrated $SbOReO_4 \cdot 2H_2O$ for the oxidation of ethanol and the aldol condensation of acetone is consistent with acidic behavior. Crystal data: $SbOReO_4 \cdot 2H_2O$, M_r = 423.98, orthorhombic, space group *Pbca* (No. 61), a = 5.6952 (5) Å, b = 18.325 (2) Å, c = 11.909 (1) Å, V = 1242.9 (3) Å^3, Z = 8, T = 298 K. Final residuals of R_p = 1.43% and R_{wp} = 1.84% (χ^2 = 1.24) were obtained for 58 parameters and 2600 data points (powder neutron diffraction data).

Introduction

Layered inorganic materials are of great interest with respect to their novel properties in such diverse areas as anisotropic electronic/ionic conduction, intercalation, ion-exchange, and catalysis.[1] A notable example is $VOPO_4 \cdot 2H_2O$,[2] which undergoes a novel redox/intercalation reaction,[3] leading to new phases such as $Na_{1/2}VOPO_4 \cdot 2H_2O$.[4] Other related phases, such as α-$VO(HPO_4) \cdot 2H_2O$[5] and β-$VO(HPO_4) \cdot 2H_2O$,[6] have recently been prepared (and characterized by *ab initio* structure determination) in the same system, showing the variety of structures possible in related, layered materials built up from the same structural motifs. Interlayer hydrogen bonding appears to be a key structural feature of all of these layered, hydrated V/P/O compounds, and determination of proton locations is a key to fully understanding the interlayer bonding forces in these materials. Because hydrogen-atom positions may be ambiguous from standard X-ray single-crystal studies, neutron powder diffraction has proved an important technique for full structural determination of these phases. Thus, the full structure, including deuteron locations, of $VOPO_4 \cdot 2D_2O$[7] was determined by the Rietveld method. Despite the very large incoherent scattering component of protons, which has traditionally militated against neutron powder diffraction studies of hydrogenous materials, the full structure of as-synthesised α-$VO(HPO_4) \cdot 2H_2O$[5] has recently been established from profile refinement against powder neutron data.

As far as we can ascertain, there is no literature on the Sb/Re/O and related systems, except for reports concerning the preparation of the perovskite-type mixed oxides $\sim Ba_6ReSb_2O_{14.5}$[8] and Ba_3ReSbO_9[9] at high temperatures. Conversely, the analogous Bi/Re/O system has been studied in some detail,[10-12] and several ternary oxides of this general type have proved to be excellent catalysts in partial

• Abstract published in *Advance ACS Abstracts*, September 15, 1993.

(1) *Crystallography and Crystal Chemistry of Materials with a Layered Structure*; Levy, F. A., Ed.; D. Reidel: Boston, 1975.
(2) Tietze, H. R. *Aust. J. Chem.* **1981**, *34*, 2035.
(3) Johnson, J. W.; Jacobson, A. J. *Angew. Chem., Int. Ed. Engl.* **1983**, *22*, 412.
(4) Wang, S. L.; Kang, H. Y.; Cheng, C. Y.; Lii, K. H. *Inorg. Chem.* **1991**, *30*, 3496.
(5) Le Bail, A.; Ferey, G.; Amoros, P.; Beltran-Porter, D. *Eur. J. Solid State Inorg. Chem.* **1989**, *26*, 419.
(6) Le Bail, A.; Ferey, G.; Amoros, P.; Beltran-Porter, D.; Villeneuve, G. *J. Solid State Chem.* **1989**, *79*, 169.
(7) Tachez, M.; Theobald, F.; Bernard, J.; Hewat, A. W. *Rev. Chim. Miner.* **1982**, *19*, 291.
(8) Kemmler-Sack, S.; Ehmann, A. *Z. Anorg. Allg. Chem.* **1981**, *483*, 161.
(9) Kemmler-Sack, S.; Treiber, U. *Z. Anorg. Allg. Chem.* **1982**, *484*, 173.
(10) Rae-Smith, A. R.; Cheetham, A. K. *J. Solid State Chem.* **1979**, *30*, 345.
(11) Cheetham, A. K.; Rae-Smith, A. R. *Mater. Res. Bull.* **1981**, *16*, 7.
(12) Cheetham, A. K.; Rae-Smith, A. R. *Acta Crystallogr.* **1985**, *B41*, 225.

0897-4756/93/2805-1631$04.00/0

oxidation reactions.[13,14] The title compound was prepared during exploratory hydrothermal synthesis of the Sb/Re/O system, and the full crystal structure, including proton positions, has been determined from powder neutron diffraction data. In light of the important catalytic reactions of dehydrated $VOPO_4$-type materials,[15] we have also screened the catalytic activity of dehydrated $SbOReO_4{\cdot}2H_2O$ for partial oxidation reactions.

Experimental Section

Sample preparation: The synthesis of $SbOReO_4{\cdot}2H_2O$ was carried out hydrothermally. Antimony powder was treated with perrhenic acid (90%) at 250 °C and 70 atm for 24 h to yield a biphasic solid product. Colorless platelike crystals of the title compound were readily separated from a black, microcrystalline powder. Subsequently, a method for the preparation of a pure, microcrystalline sample of $SbOReO_4{\cdot}2H_2O$ was devised as follows: an aqueous solution of perrhenic acid (85%) and Sb_2O_3 was refluxed for 2 days. The resulting slurry was then transferred to a Teflon-lined Parr hydrothermal bomb which was sealed and heated to 200 °C for 24 h. Upon opening the bomb, needle-shaped crystals were observed in a rust-colored liquid. On standing for several days, the solution turned into a solid white mass. The powder X-ray diffraction pattern of the dried material indicated that it was pure $SbOReO_4{\cdot}2H_2O$. Over several weeks at room temperature, this material partially decomposed to ReO_2 and other, unidentified phases.

Powder X-ray data for $SbOReO_4{\cdot}2H_2O$ were collected on a computer-controlled Phillips powder diffractometer (Cu Kα radiation, λ = 1.541 78 Å). The powder pattern of pure $SbOReO_4{\cdot}2H_2O$ could be indexed on the basis of the single-crystal unit cell constants determined below. Thermogravimetric analysis on $SbOReO_4{\cdot}2H_2O$ was carried out using a du Pont 9900 system, using a heating rate of 10 °C/min in flowing N_2 gas. Infrared spectra of $SbOReO_4{\cdot}2H_2O$ were recorded on a Perkin-Elmer 1710 FTIR spectrometer; samples were diluted with 95% KCl.

Structure determination: Approximate heavy atom positions in the $SbOReO_4{\cdot}2H_2O$ structure were elucidated by single-crystal X-ray diffraction methods: graphite-monochromated Mo Kα radiation, λ = 0.710 73 Å; Enraf-Nonius CAD4 diffractometer; crystal size 0.20 × 0.75 × 0.03 mm; refined orthorhombic cell parameters: a = 5.690 (5), b = 18.307 (8), c = 11.900 (4) Å; space group (from systematic absences) *Pbca* (No. 61); structure solution with SHELXS-86; refinement software: CRYSTALS. Approximate Sb-, Re-, and O-atom positions were established, but the refinement was unable to reveal the hydrogen-atom positions due to severe absorption effects.

Powder neutron diffraction: The complete crystal structure of $SbOReO_4{\cdot}2H_2O$ was determined by Rietveld refinement, using constant-wavelength neutron powder diffraction data (λ = 1.5946 Å). A pure, well-ground sample of $SbOReO_4{\cdot}2H_2O$ was loaded into a cylindrical vanadium can, and room-temperature data were collected using the high-resolution powder diffractometer, D2b, at the Institut Laue-Langevin, Grenoble, France. Data were collected over an angle range of 10–145°, with a step size of 0.05°. Before profile refinement, the raw data were collated and normalized using local software routines.

Rietveld refinement was carried out using the program GSAS.[16] The starting atomic model [Sb, Re, O sites: space group *Pbca* (No. 61)] was taken from the single-crystal X-ray study. Coherent neutron-scattering lengths ($\times 10^{-14}$ m) were assigned as follows: b(Sb) = 0.564, b(Re) = 0.920, b(O) = 0.581, b(H) = −0.374. The usual "profile" parameters (scale factor, background polynomial values, zero-point error, Gaussian peak-shape width variation descriptors, lattice parameters), atomic positional, and atom-type isotropic thermal parameters were added as variables to the refinement process in the usual fashion. The thermal factors of Sb and Re were also constrained to be equal. After stable convergence was achieved, the four proton sites were located from Fourier difference maps and added to the atomic model. Further cycles of least-squares refinement led to final residuals of R_p = 1.43% and R_{wp} = 1.84% (χ^2 = 1.24) for 58 parameters and 2600 data points. No account was taken of any uncertainty in the incident neutron wavelength in the least-squares calculations. Crystallographic details for $SbOReO_4{\cdot}2H_2O$ are summarized in Table I, and the final observed, calculated and difference profile plots are illustrated in Figure 1.

Table I. Crystallographic Parameters for the Powder Neutron Diffraction Study of $SbOReO_4{\cdot}2H_2O$

empirical formula	$Re_1Sb_1O_7H_4$
formula wt	423.98
crystal system	orthorhombic
a (Å)	5.6952(5)
b (Å)	18.325(2)
c (Å)	11.909(1)
V (Å^3)	1242.9(3)
Z	8
space group	*Pbca* (No. 61)
T (K)	298(2)
ρ_{calc} (g/cm^3)	4.531
powder data points	2600
parameters	58
R_p[a] (%)	1.43
R_{wp}[b] (%)	1.84
χ^2	1.24

[a] $R_p = \Sigma|y_o - Cy_c|/\Sigma|y_o|$. [b] $R_{wp} = [\Sigma w(y_o - Cy_c)^2/\Sigma w y_o^2]^{1/2}$, where C is a scale factor.

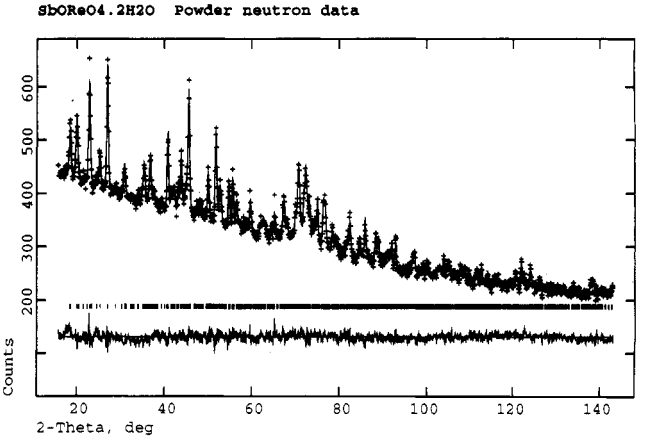

Figure 1. Final observed data (crosses), calculated (line) and difference profile plots for $SbOReO_4{\cdot}2H_2O$. Allowed reflection positions are indicated by tick marks. The large background due to incoherent scattering from the protons is evident.

Catalytic studies: the effect of (dehydrated) $SbOReO_4{\cdot}2H_2O$ on oxidation reactions at 300 °C and ambient pressure was studied using a plug-flow microreactor which was heated in an electric tube furnace. The catalyst (3 mL) was packed in a quartz tube with glass wool plugs at either end. Brooks 5850 mass flow controllers monitored gases flowing into the reactor, and liquids were metered using a Harvard syringe pump. The product stream passed through a heated sample loop connected to a Hewlett-Packard 5890 gas chromatograph, thus enabling product analysis. The chromatograph was fitted with a FID and a 6-ft, 1/8-in. inside diameter gas chromatograph 220 packed stainless steel column (80/100 mesh) from Alltech. The gas sample was injected using a 6-port Carle high temperature valve with a 0.25-mL sample loop. A typical program was 50 °C, hold 4 min, ramp at 8 °C/min to 200 °C, hold 4 min. Helium was used as the carrier gas.

Results

Physical data: TGA of $SbOReO_4{\cdot}2H_2O$ (Figure 2) indicated a two-step dehydration process, corresponding

(13) Centri, G.; Trifiro, F. *Catal. Rev. Sci. Eng.* **1986**, *28*, 165.
(14) Graselli, R. K.; Burrington, J. D. *Adv. Catal.* **1981**, *30*, 133.
(15) Centri, G. *Catal. Today* **1991**, *16*, 5.
(16) Von Dreele, R. B.; Larson, A. C. GSAS User Guide, Los Alamos National Laboratory, Los Alamos, NM, 1990.

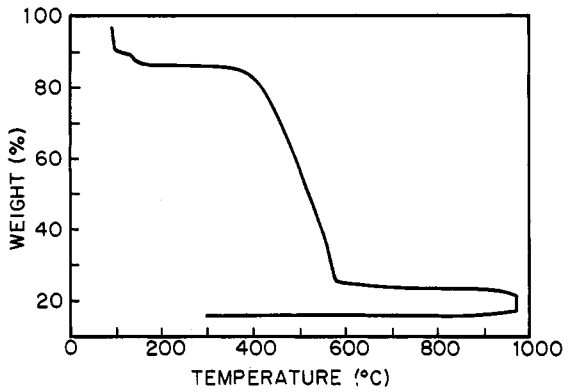

Figure 2. Thermogravimetric analysis plot for $SbOReO_4 \cdot 2H_2O$.

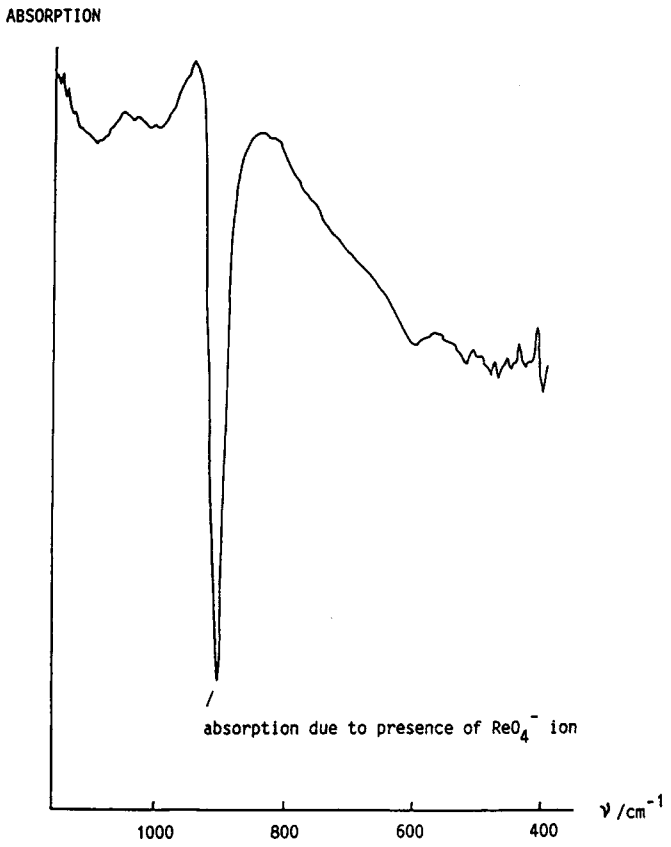

Figure 3. IR spectrum of $SbOReO_4 \cdot 2H_2O$, showing the intense 918 cm^{-1} characteristic absorption band of the ReO_4^- group.

to complete water loss, beginning at 60 °C and completed by 160 °C. However, the two water molecules are not lost in a simple 1:1 ratio. In the range 370–570 °C, a significant weight loss occurs corresponding to the sublimation of Re_2O_7 from the sample. IR data for $SbOReO_4 \cdot 2H_2O$ (Figure 3) indicated the presence of hydrogen-bonded water molecules: sharp bands at 3600 and 1200 cm^{-1} and a broad maximum at 3400 cm^{-1} were apparent. An intense absorption at 918 cm^{-1} may be attributed to the ReO_4^- group.[17]

Crystal structure: Final atomic positional and thermal parameters for $SbOReO_4 \cdot 2H_2O$ are shown in Table II, with selected bond distance/angle data in Tables III and IV, respectively. $SbOReO_4 \cdot 2H_2O$ forms a new crystal structure, built up from SbO^+ and ReO_4 subunits, forming $SbOReO_4 \cdot H_2O$ layers, interconnected by a H-bonding layer

(17) Müller, A.; Krebs, B. *J. Mol. Spectrosc.* **1967**, *24*, 180.

Table II. Atomic Positional Parameters for $SbOReO_4 \cdot 2H_2O$

atom	x	y	z	U_{iso} (Å²)
Sb(1)	0.5154(26)	0.9123(6)	0.3427(7)	0.017(2)
Re(1)	0.5077(14)	0.0798(4)	0.1242(5)	0.017(2)
O(1)	0.6214(20)	0.0094(7)	0.2039(10)	0.023(2)
O(2)	0.7168(22)	0.1202(7)	0.0416(10)	0.023(2)
O(3)	0.3851(22)	0.1463(6)	0.2130(11)	0.023(2)
O(4)	0.2896(22)	0.0455(6)	0.0416(10)	0.023(2)
O(5)	0.3233(20)	0.8713(6)	0.2227(9)	0.023(2)
O(6)	0.4626(19)	0.7991(5)	0.4076(9)	0.023(2)
O(7)	0.0214(23)	0.7507(7)	0.3779(10)	0.023(2)
H(1)	0.496(5)	0.7872(10)	0.4926(14)	0.041(3)
H(2)	0.3011(33)	0.7845(11)	0.3883(18)	0.041(3)
H(3)	−0.0685(35)	0.7901(11)	0.3425(17)	0.041(3)
H(4)	0.020(4)	0.7150(11)	0.3220(17)	0.041(3)

Table III. Bond Distances (Å) for $SbOReO_4 \cdot 2H_2O$

Sb(1)–O(1)	2.502(17)	Sb(1)–O(1)′	2.917(17)
Sb(1)–O(2)	2.879(16)	Sb(1)–O(5)	1.950(16)
Sb(1)–O(5)′	2.061(17)	Sb(1)–O(6)	2.234(15)
Re(1)–O(1)	1.728(14)	Re(1)–O(2)	1.713(13)
Re(1)–O(3)	1.758(13)	Re(1)–O(4)	1.704(13)
O(6)–H(1)	1.053(22)	O(6)–H(2)	0.985(25)
O(7)–H(3)	0.981(26)	O(7)–H(4)	0.933(26)
H(1)···O(7)[a]	1.698(23)	H(2)···O(7)[a]	1.714(24)
H(3)···O(5)[a]	1.788(24)	H(4)···O(3)[a]	1.888(24)

[a] The dots refer to a hydrogen-bond linkage.

Table IV. Bond Angles (deg) for $SbOReO_4 \cdot 2H_2O$

O(1)–Sb(1)–O(1)′	68.0(4)	O(1)–Sb(1)–O(2)	124.2(6)
O(1)–Sb(1)–O(5)	85.7(5)	O(1)–Sb(1)–O(5)	78.7(6)
O(1)–Sb(1)–O(6)	157.1(6)	O(1)–Sb(1)–O(2)	133.6(5)
O(1)–Sb(1)–O(5)	70.4(6)	O(1)–Sb(1)–O(5)	143.6(6)
O(1)–Sb(1)–O(6)	121.9(6)	O(2)–Sb(1)–O(5)	145.1(7)
O(2)–Sb(1)–O(5)	77.6(5)	O(2)–Sb(1)–O(6)	66.1(5)
O(5)–Sb(1)–O(5)′	93.4(5)	O(5)–Sb(1)–O(6)	79.6(6)
O(5)–Sb(1)–O(6)	84.6(6)		
O(1)–Re(1)–O(2)	112.2(7)	O(1)–Re(1)–O(3)	109.6(5)
O(1)–Re(1)–O(4)	108.4(7)	O(2)–Re(1)–O(3)	108.8(7)
O(2)–Re(1)–O(4)	109.6(6)	O(3)–Re(1)–O(4)	108.2(8)
Re(1)–O(1)–Sb(1)	143.5(7)	Re(1)–O(1)–Sb(1)	129.7(6)
Sb(1)–O(1)–Sb(1)′	83.0(5)	Re(1)–O(2)–Sb(1)	138.7(7)
Re(1)–O(3)–H(4)	139.6(11)	Sb(1)–O(5)–Sb(1)′	127.9(8)
Sb(1)–O(5)···H(3)[a]	116.5(9)	Sb(1)–O(5)···H(3)[a]	115.6(8)
Sb(1)–O(6)–H(1)	120.0(11)	Sb(1)–O(6)–H(2)	107.3(13)
H(1)–O(6)–H(2)	109.6(18)	H(1)···O(7)···H(2)[a]	99.3(14)
H(1)···O(7)–H(3)[a]	130.3(17)	H(1)···O(7)–H(4)[a]	111.2(15)
H(2)···O(7)–H(3)[a]	104.5(15)	H(2)···O(7)–H(4)[a]	108.4(18)
H(3)–O(7)–H(4)	101.8(18)		
O(6)–H(1)···O(7)[a]	166.9(16)	O(6)–H(2)···O(7)[a]	169.4(20)
O(5)···H(3)–O(7)[a]	168.4(19)	O(3)···H(4)–O(7)[a]	162.7(21)

[a] The dots refer to a hydrogen-bond contact.

of water molecules. There are 13 asymmetric atoms: one antimony cation (distorted 6-coordinate), one rhenium cation (tetrahedral), seven oxygen anions (various coordinations: see below) and four protons (parts of water molecules). The crystal structure of $SbOReO_4 \cdot 2H_2O$ is illustrated in Figure 4 using ORTEP.[18]

The Sb^{III}-cation environment (Figure 5) cannot be well described by any simple, regular polyhedron. There are six Sb–O vertices, the three shortest of which [O(5), O(5)′, O(6), Table III] form a very-distorted trigonal pyramid with the antimony atom. Here, O(6) is part of a water molecule. Distorted 6-fold coordination is completed by longer bonds to O(1), O(1)′, and O(2). This distortion is probably caused by the (unobserved) electron lone pair of the Sb^{III} species. An average Sb–O distance of 2.42 Å results. The Re^{VII} species forms a typical, regular tetrahedron with four oxygen-atom neighbors; d_{av}(Re–O) =

(18) Johnson, C. K. Report ORNL-5138, Oak Rdige National Laboratory, TN, 1976, with local modifications.

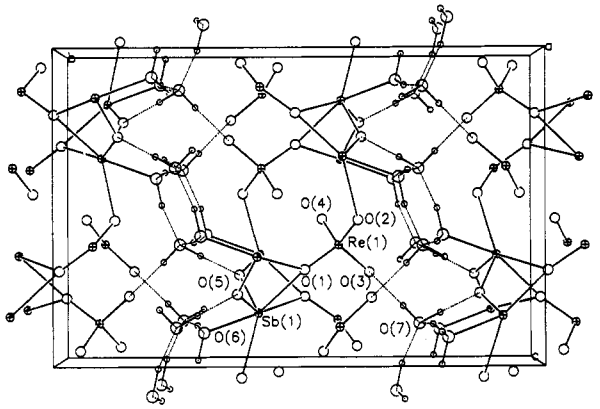

Figure 4. Crystal structure of $SbOReO_4 \cdot 2H_2O$, viewed down the *a* direction, showing the infinite $SbOReO_4 \cdot H_2O$ layers, separated by sheets of water molecules. Arbitrary atomic radii: Sb atoms indicated as "filled" circles, Re atoms as "open" circles, O atoms as plain circles, H atoms as small, plain circles. H bonds are indicated by dotted lines, and selected non-hydrogen atom are labeled.

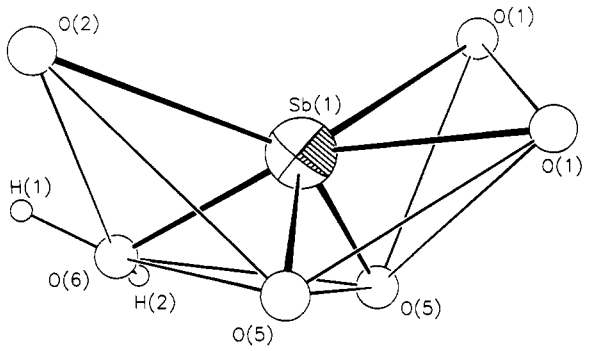

Figure 5. Irregular Sb-atom coordination in $SbOReO_4 \cdot 2H_2O$: thin lines indicate O···O contacts <4.0 Å. Arbitrary atom radii.

1.725 (7) Å, compared to an expected ionic-radii-sum distance of 1.74 Å.[19]

The oxygen-atom species adopt various bonding environments: O(1) bridges two Sb atoms and one Re atom, O(2) bonds to one Re and one Sb neighbor, O(3) and O(4) bond only to Re and O(5) is the short, "antimonyl" bridging oxygen atom between adjacent antimony atoms. Both Sb–O(5) bonds are approximately the same length (~1.97 Å), and the characteristic short/long bond-length alternation observed in some M–O–M–O chains, for example the "titanyl" chain in $KTiOPO_4$,[20] is not observed in $SbOReO_4 \cdot 2H_2O$. Of the two water molecules, the first [atoms O(6), H(1) and H(2)] is involved in a Sb–O bond, and the second [atoms O(7), H(3), and H(4)] occupies the interlayer region (vide infra) and bonds to neither Sb nor Re. The average O–H bond distance of 0.99 (2) Å is in good agreement with that found in other neutron-diffraction studies of O–H species in similar systems.[7]

The Sb/Re/O layer structure of $SbOReO_4 \cdot 2H_2O$, which is orientated in the (101)-crystallographic plane, is shown in more detail in Figure 6. Infinite, zigzag –Sb(1)–O(5)–Sb(1)–O(5)– chains (all O–Sb–O angles cis with respect to the Sb center) propagate in the *a* direction, and a second inter-Sb link is made via O(1), which also bonds to Re(1). The sheet connectivity is completed by the ReO_4 group,

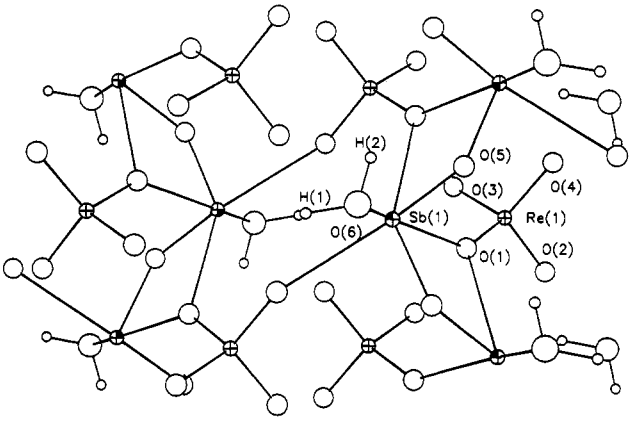

Figure 6. Detail of the infinite layer structure in $SbOReO_4 \cdot 2H_2O$, viewed in the [101] projection, showing the infinite –Sb–O–Sb–O– chains, interconnected by ReO_4 groups. Atom radii are arbitrary, and O(7), H(3), and H(4) are omitted for clarity.

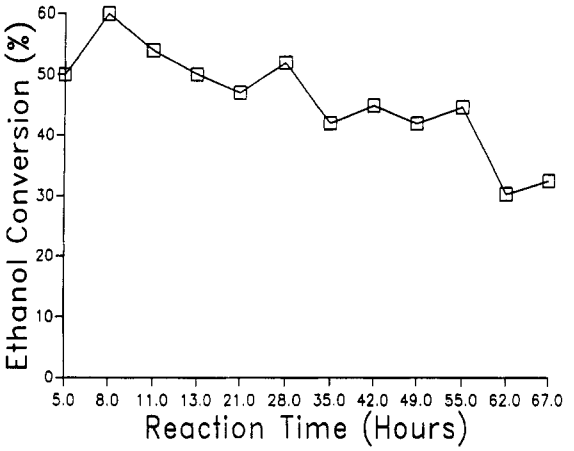

Figure 7. Plot of ethanol oxidation conversion as a function of time on stream for dehydrated $SbOReO_4 \cdot 2H_2O$.

which bridges adjacent antimony/oxygen strings via O(1)–Re(1)–O(2)–Sb(1) linkages.

All four protons are involved in H bonds, which connect adjacent sheets into a three-dimensional structure. Both the protons connected to O(6) make H bonds to (different) O(7) species, in the interlayer region, which results in approximately "tetrahedral" geometry around O(7). The two protons attached to O(7) make H bonds to O atoms in adjacent Sb/Re/O layers, as O(5)···H(3)–O(7)–H(4)···O(3), completing the structure. The average O···H H-bond distance (1.77 Å) and O–H···O angle (167°) are typical.

Catalytic results: Ethanol oxidation was monitored by passing a mixture of 8% oxygen/nitrogen and ethanol over the catalyst bed. The average conversion of ethanol ranged from ~30–50%, depending on the time on stream, as shown in Figure 7. Some variations were observed, but the general trend was an initial increase in conversion from 50 to 60%, followed by a slow decrease over 60 h to the low 30% level. The product distribution was as follows, in order of decreasing concentration: ethyl acetate, acetaldehyde, diethyl ether, ethyl butyrate and smaller amounts of ethylene. Figure 8 shows how the selectivities change versus time on stream.

For the aldol condensation of acetone, a mixture of acetone and nitrogen was passed over the fresh catalyst bed: the conversion of acetone was ~20%. The major products were mesityl oxide, isophorone, mesitylene and xylenes, in order of decreasing selectivity. No activity

(19) Shannon, R. D. *Acta Crystallogr.* **1976**, *A32*, 751.
(20) Stucky, G. D.; Phillips, M. L. F.; Gier, T. E. *Chem. Mater.* **1989**, *1*, 492.

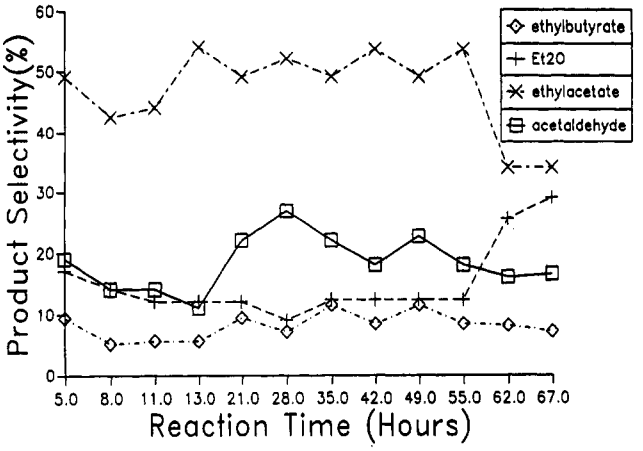

Figure 8. Plot of ethanol oxidation selectivity for various products versus time on stream for dehydrated $SbOReO_4{\cdot}2H_2O$.

was observed for the following reactions: gas phase oxidation of toluene, *p*-xylene, propylene and butene. Slight activity was seen for the dehydrogenation of *p*-cymene to *p*-methyl-α-methylstyrene.

The used catalyst had no crystalline $SbOReO_4{\cdot}2H_2O$ present; only ReO_2 and Sb_2O_3 could be positively identified in the complex powder X-ray diffraction pattern of the residual material. Since the rate of decomposition of the starting compound during the reaction is unknown, the catalytically active species could be either $SbOReO_4$, the dehydrated form of the title compound, the decomposition products ReO_2 or Sb_2O_3, or a combination thereof. The decomposition reaction may be formally written as

$$2SbOReO_4{\cdot}2H_2O \rightarrow 2ReO_2 + Sb_2O_3 + 3/2O_2 + 4H_2O$$

The product distribution suggests that the active sites in the catalyst are acidic, in spite of the fact that the antimony cation has a lone pair of electrons that could be basic.

Conclusions

The new layered material $SbOReO_4{\cdot}2H_2O$ has been prepared and characterized. Powder neutron diffraction was successful in locating the proton sites in the as-synthesized hydrogenous compound, allowing the full details of the interlayer H-bonding scheme to be elucidated. The success of this and other studies emphasizes that proton location in moderately complex hydrogenous materials may be successfully accomplished by using powder neutron diffraction methods.[7,21]

Acknowledgment. We thank K. J. Thrash (Amoco) for technical assistance with the synthesis and catalytic screening and R. J. B. Jakeman for help with the X-ray single-crystal measurements. A.V.P.M. is grateful to Amoco Chemical Co. for the provision of a studentship, and we thank the Science and Engineering Research Council (UK) for the provision of neutron diffraction facilities at ILL, Grenoble.

(21) Newsam, J. M. *J. Chem. Soc., Chem. Commun.* **1986**, 1295.